Possibility of Prolific Pair Production with High-Power Lasers

A. R. Bell

Clarendon Laboratory, University of Oxford, Parks Road, Oxford OX1 3PU, United Kingdom
and STFC Central Laser Facility, RAL, Didcot, OX11 0QX, United Kingdom

John G. Kirk

Max-Planck-Institut für Kernphysik, Saupfercheckweg, 1, D-69117, Heidelberg, Germany

Prolific electron-positron pair production is possible at laser intensities approaching 10^{24} W cm^{-2} at a wavelength of 1 μm. An analysis of electron trajectories and interactions at the nodes ($B = 0$) of two counterpropagating, circularly polarized laser beams shows that a cascade of γ rays and pairs develops. The geometry is generalized qualitatively to linear polarization and laser beams incident on a solid target.

High-power laser facilities have made dramatic progress recently, and the next few years may bring intensities of 10^{23}–10^{24} W cm^{-2} within reach. This naturally opens up new physics regimes [1,2]. The relativistic Lorentz factor of an electron oscillating in vacuum in the electromagnetic field of a planar linearly polarized laser beam is $860(I_{24}\lambda_{\mu m}^2)^{1/2}$ where I_{24} is the laser intensity in 10^{24} W cm^{-2} and $\lambda_{\mu m}$ is the laser wavelength in micron. The corresponding peak electric and magnetic fields are $2.7 \times 10^{15}I_{24}^{1/2}$ V m^{-1} and $91I_{24}^{1/2}$ GG. The Schwinger field $E_{\text{crit}} = 1.3 \times 10^{18}$ V m^{-1} required for spontaneous electron-positron pair creation out of the vacuum would be attained at a laser intensity of 2.3×10^{29} W cm^{-2} [3,4]. Although this interesting regime is still far beyond projected laser intensities, several other strong-field QED effects will soon be accessible to experiment. In this Letter we show how copious pair production by accelerated electrons interacting with the laser field can be achieved using laser intensities $\sim 10^{24}$ W cm^{-2}. The key is to exploit the large transverse electromagnetic field seen by an electron when it experiences laser beams that are not propagating in parallel. We illustrate this effect by computing the case of counterpropagating, circularly polarized beams. The advantage offered by this configuration is analogous to the dramatic increase in center-of-mass energy when using colliding particle beams instead of stationary targets. We argue that this advantage remains in less specific configurations such as tight focus and reflection from a solid surface. Consequently, it may be possible to convert a large fraction of the laser energy into electron-positron pairs at a laser intensity of $\sim 10^{24}$ W cm^{-2} at approximately solid plasma density.

Relativistic electrons with Lorentz factor γ moving perpendicular to a homogeneous magnetic field B produce pairs if $\gamma B/B_{\text{crit}}$ is greater than or of the order of unity, where, $B_{\text{crit}} = 4.414 \times 10^4$ GG is the magnetic equivalent of the Schwinger field E_{crit}. The cross sections for this and other relevant processes are well known [5] and of interest

also in astrophysics [6]. Provided the electron trajectory can be approximated classically, these rates, when computed in a frame in which $\boldsymbol{E} \times \boldsymbol{B} = 0$, are functions of the electric and magnetic fields only in the combination $E^2 + B^2$ [7,8]. Therefore, in a homogeneous electric field $\hat{\boldsymbol{e}}E$, pair production occurs if the parameter

$$\eta = \frac{\gamma E \sin\theta}{E_{\text{crit}}} \tag{1}$$

is of order unity or larger, where θ is the angle between the electric field and the electron momentum. Pair production by the trident process in which the electric field is provided by a high-Z nucleus and the Lorentz factor by accelerating electrons in the laser field, has already been observed, but the process is relatively inefficient, and the yield achieved was 10^{-4} positrons for each fast electron [9–11]. Electron-positron pairs have also been produced by colliding 46.6 GeV electrons from a linear accelerator with an opposing laser beam, but this produced a relatively modest number of pairs [12].

In a strong electromagnetic wave in vacuum, the Lorentz factor of an electron oscillates about a value roughly equal to the strength parameter of the wave [13]

$$a = \frac{eE\lambda}{2\pi mc^2} = 8.4 \times 10^2(I_{24}\lambda_{\mu m}^2)^{1/2}, \tag{2}$$

so that η in Eq. (1) is approximately $1.7I_{24}\lambda_{\mu m}$. This looks promising at first sight. However, Eq. (1) assumes that $eE \sin\theta$ is the component of the particle's acceleration perpendicular to its velocity, which is not the case in a laser field. In reality, an electron that is picked up by a single laser beam at initially low energy in the laboratory is accelerated on a trajectory that severely reduces the effective value of η below that in Eq. (1), because the electric force is almost precisely canceled by that exerted by the magnetic field.

This can be understood in a way that brings out the analogy with particle accelerators. In a plane electromag-

netic wave in vacuum a charged particle has a periodic trajectory in one special frame of reference (ignoring for the moment radiation reaction) [13]. This frame can be called the zero momentum frame (ZMF). In it, all of the particle's phase-space variables are strictly periodic at the period of the wave, independently of its polarization and waveform, and the particle energy oscillates around a value $\gamma mc^2 \approx amc^2$. In this frame, the electric and magnetic forces do not, in general, cancel, and the perpendicular component of the acceleration is well approximated by eE', where E' is the field strength of the wave measured in the ZMF. Thus, the importance of strong-field QED effects, such as pair creation, is indeed determined by the parameter η, as defined in Eq. (1), but computed in the ZMF, i.e., $\eta \approx aE'/E_{\rm crit}$. In the case of a single laser beam hitting a particle at rest, the ZMF does not coincide with the laboratory frame, because the particle recoils. In fact, the ZMF moves in the direction of propagation of the laser beam with a velocity corresponding to a Lorentz factor equal to a [13]. The laser frequency in the ZMF is thus redshifted compared to the laboratory frame. Because the strength parameter a is a Lorentz invariant, the reduced wave frequency in the ZMF implies a reduced amplitude of the wave field: $E' \approx E/a$. Consequently the (Lorentz invariant) criterion for the importance of strong-field QED effects becomes $aE'/E_{\rm crit} \approx E/E_{\rm crit} > 1$. In other words, by using a single laser beam, the advantage gained over pure vacuum effects by the relativistic oscillation of the electron is lost.

This is a consequence of the dual roles of accelerator and target that are played by the laser beam. If the electron, instead of being initially at rest, is initially moving with a Lorentz factor $\gamma_{\rm init}$ that is much larger than the strength parameter of the laser beam, as in the experiment of Burke *et al.* [12], the ZMF moves with almost the speed of the electron, and $\eta \approx \gamma_{\rm init} E \sin\theta/E_{\rm crit}$. The initial Lorentz factor of the electron contributes to the threshold condition, but the Lorentz factor due to oscillation in the laser field does not. In this case the laser plays only the role of the target.

However, as in the case of intersecting particle beams, the situation can be rescued if counterpropagating laser beams are employed. Then the ZMF coincides with the laboratory frame, and the importance of strong-field QED is again determined by Eq. (1). A similar benefit is gained with a laser beam in tight focus—which can be decomposed into obliquely propagating plane waves—or with a beam in which a standing wave is set up when the laser encounters a dense plasma. Experimentally, some of the most promising cases involve laser-solid interactions, but the analysis of these is complicated. Instead, we consider the theoretically simple case of pair production at the nodes ($B = 0$) of two counterpropagating circularly polarized laser beams of equal intensity. The argument can then be qualitatively generalized to laser-solid interactions.

Strong-field QED effects at the nodes of counterpropagating waves have been considered previously [14,15], but only for a vacuum in which the threshold condition relates to E rather than γE.

Classically, the electron equation of motion, including radiation reaction according to the Landau-Lifshitz prescription [16], is

$$\frac{d(\gamma\boldsymbol{\beta})}{dt} = -\frac{e}{m_e c}(\boldsymbol{E} + \boldsymbol{\beta} \times \boldsymbol{B}) - \frac{2e^4\gamma^2}{3m^3c^5}\boldsymbol{\beta}|\boldsymbol{E} + \boldsymbol{\beta} \times \boldsymbol{B}|^2_\perp. \quad (3)$$

The terms that have been omitted here are of order γ^{-2}. The final term of Eq. (3) represents the drag and energy loss due to radiative emission, to which pair production is related, and is proportional to the square of that component of the Lorentz force $\boldsymbol{E} + \boldsymbol{\beta} \times \boldsymbol{B}$ perpendicular to $\boldsymbol{\beta}$. In the case of a planar unidirectional wave, the reduction in the electric field in the ZMF is equivalent to the near cancellation of $\boldsymbol{E}$ with $\boldsymbol{\beta} \times \boldsymbol{B}$ in the laboratory frame.

Two counterpropagating laser beams produce a standing wave with nodes at which $B = 0$ and the electric field rotates in direction with constant amplitude. By symmetry, an electron placed exactly at the node does not move in the direction of the waves, but performs circular motion with the centripetal force provided by the electric field. The equation of motion (3) then simplifies to

$$\frac{d(\gamma\boldsymbol{\beta})}{dt} = \frac{eE}{mc}\left\{-\hat{\boldsymbol{e}} - \frac{2}{3}\boldsymbol{\beta}\gamma^2\frac{E}{E_{\rm cl}}[1 - (\boldsymbol{\beta}\cdot\hat{\boldsymbol{e}})^2]\right\}, \quad (4)$$

where $\hat{\boldsymbol{e}}$ is the unit vector in the direction of the electric field and we have defined the characteristic value $E_{\rm cl}$ of the electric field in classical electrodynamics: $E_{\rm cl} = m^2c^4/e^3 = E_{\rm crit}/\alpha_f$ (α_f is the fine-structure constant). As can be seen from Eq. (4), the radiation reaction force becomes important when $\gamma^2 E/E_{\rm cl} \sim 1$, i.e., $\eta \sim (\gamma\alpha_f)^{-1}$, a situation that is reached at laser intensities $\sim 10^{23}\lambda_{\mu{\rm m}}^{-4/3}$ W cm^{-2}. The Landau-Lifshitz prescription for the radiation reaction term is valid up to $\eta \approx 1/\alpha_f$ [17] but quantum effects already intervene at $\eta \sim 1$ [5].

Within a small fraction of a laser period, the electron trajectory described by Eq. (4) adjusts itself such that the component of electric field parallel to $\boldsymbol{\beta}$ precisely compensates the radiative losses, while the perpendicular component enforces circular motion at the laser period, with Lorentz factor $\gamma = a\sin\theta$. Combining these, and using the definition (1) of the threshold parameter we can express E in terms of η. In an underdense plasma, the total electric field E is related to the intensity I of each laser beam (separately) by $I = cE^2/(16\pi)$, which gives

$$I_{24} = 2.75\eta^4 + 0.28(\eta/\lambda_{\mu{\rm m}}). \quad (5)$$

This relation is plotted in Fig. 1 for a laser of wavelength 1 μm. In terms of these parameters, $\sin\theta = 0.53\sqrt{\eta}(I_{24}\lambda_{\mu{\rm m}})^{-1/2}$—at low intensity, the particle moves
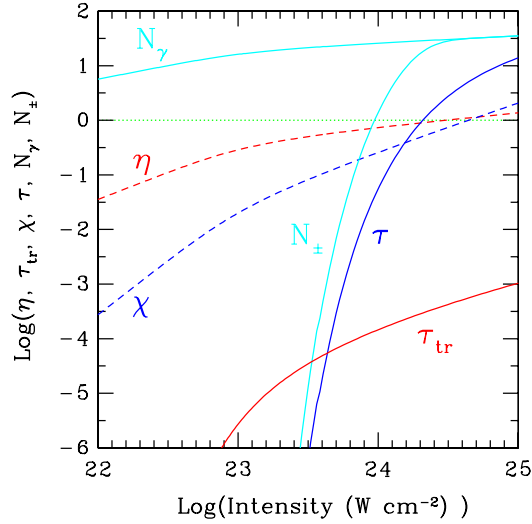
FIG. 1 (color online). The parameters η and χ—see Eqs. (1) and (7)—controlling the importance of electromagnetic conversion by the accelerated electron and its curvature photon, respectively, as a function of laser intensity, for a laser wavelength of 1 μm. Also plotted are the optical depth τ of the curvature photon across one wavelength, the number $N_\pm$ of pairs produced per electron in one laser period by both this process and by that of pair production by the trident process—labeled τ_{tr}, and the number N_γ of curvature radiation photons produced per electron per laser period.

almost exactly perpendicularly to E and η rises linearly with the laser intensity. However, when radiation reaction becomes important, this rise is slowed, and $\eta = 1$ is not achieved until $I_{24} = 3$. The photons radiated because of the acceleration of the electron in the electric field of the laser—which we term *curvature radiation* [18]—can be described classically using the theory of synchrotron radiation. This predicts that most radiated photons are emitted with an energy

$$h\nu_s = 0.44\eta\gamma mc^2, \qquad (6)$$

where $\gamma mc^2 = 328\sqrt{\eta\lambda_{\mu m}}$ MeV is the energy of the relativistic electron. Because of quantum effects analogous to the Klein-Nishina corrections to the Thomson cross section [5,19], the radiative energy loss does not proceed in the continuous manner implied by Eq. (4) when $\eta > 1$ and $I_{24} \gg 1$. Nevertheless, the classical trajectory is an adequate approximation in the intensity range 10^{23}–10^{24} W cm^{-2}, which is of interest here, since the photon energy is significantly less than the electron energy.

However, other important quantum effects are already present at intensities in this range. There are two processes that produce electron-positron pairs. At low laser intensities, the trident process dominates, in which an electron produces an electron-positron pair via an intermediate virtual photon. In a homogeneous electric or magnetic

field (a good approximation when $\lambda_{laser} \gg h/mc = 2.4 \times 10^{-6}$ μm) the rate is given by [5,8]. Expressed as a production rate per electron per laser period, it can be written $\tau_{tr} = 0.06(I_{24}\lambda_{\mu m}^2)^{1/2}\eta^{1/4}\exp(-8/\sqrt{3\eta})$ for $\eta \ll 1$, and, for $\eta > 1$, it goes over to a slow logarithmic increase. The precise form is plotted in Fig. 1.

At higher intensities, the related process becomes important, in which the electron first produces a real photon by curvature radiation, which subsequently creates a pair. However, to compare this to the trident process one must specify the distance over which the real photon is permitted to undergo conversion: if this is large, all photons will convert into pairs, whereas if it is very short, none of them will. The two processes are almost equal in rate if, at $\eta \approx 1$, the distance is chosen to be $(\hbar/mc)(E_{crit}/E) = 1.3 \times 10^{-4}I_{24}^{-1/2}$ μm [5]. However, in reality, this length is determined by the size of the region in which the laser beams overlap, which we conservatively assume to be λ_{laser}. This gives the process that involves a real photon as intermediary a substantial advantage. An additional, though less important, advantage arises because the propagation direction of the photon does not rotate, and, therefore, the perpendicular component of electric field it experiences is $\sim E$, rather than $E\sin\theta$. The absorption coefficient is controlled by the parameter

$$\chi = \frac{h\nu_s E}{2mc^2 E_{crit}}. \qquad (7)$$

From Eq. (6) and writing E in terms of I_{24}, $\chi = 0.42\eta^{3/2}\sqrt{I_{24}\lambda_{\mu m}}$ and this function is plotted in Fig. 1. The photon optical depth to absorption in a path length λ_{laser} is $\tau = 12.8(I_{24}\lambda_{\mu m}^2)\exp[-4/(3\chi)]$, for $\chi \ll 1$, peaking at $\chi \approx 8$ and falling off for larger χ [5]. It is also plotted in Fig. 1. The total pair-production rate per electron per laser period is the product of the photon absorption probability $1 - \exp(-\tau)$ in a length λ_{laser} multiplied by the rate of production of photons by curvature radiation. This quantity, together with the number of curvature radiation photons emitted per electron per laser period (i.e., the energy radiated divided by $h\nu_s$): $N_\gamma = 6.42\alpha_f\gamma$ is also shown in Fig. 1.

Inspection of this figure shows that for laser intensities less than roughly $I = 3.3 \times 10^{23}$ W cm^{-2}, where $\eta = 0.51$, pair production is dominated by the trident process. At this intensity, each electron in the zone where the laser beams overlap produces on average 3×10^{-5} pairs in a single laser period. The curvature radiation energy losses, which are 123 kW per electron, dominate over pair production. They are sufficient to damp the laser beams in $1.8n_{23}^{-1}$ fsec where n_{23} is the electron density in 10^{23} cm^{-3}. The total number of pairs produced in the absence of other energy losses is 7×10^4 per Joule of laser energy.

At intensities above $I = 3.3 \times 10^{23}$ W cm^{-2}, the number of pairs produced by photon-induced pair production

rises steeply. These pairs are also accelerated and generate additional photons and pairs. A cascade should develop when $N_\pm \approx 1$, which occurs at $I_{24} \approx 1$ and $\eta \approx 0.7$. At this intensity, the laser power should be divided roughly equally between photons and pairs with energy ~ 80 MeV per photon and per pair. This process is not sensitive to the number of electrons initially in the interaction region. Complete conversion of laser energy to photons and pairs implies the production of $\sim 4 \times 10^{10}$ pairs per Joule of laser energy. The precise conditions under which a cascade is initiated are, however, sensitive to geometrical effects related to the intersection angle and the intersection volume of the laser beams.

For simplicity of analysis we have assessed pair production at the nodes of counterpropagating circularly polarized waves and found that the condition for pair production is $aE_\perp > E_{\text{crit}}$ where a is the strength parameter, roughly equal to the Lorentz factor of an electron oscillating in the electromagnetic wave. This contrasts with the much higher threshold in the case of an electron overtaken by a planar unidirectional wave. The unidirectional plane wave is a special case, and the conditions for prolific pair production should be met at laser intensities $\sim 10^{24}$ W cm^{-2} away from the node or when the polarization is not circular, although the analysis is more complicated and numerical factors of order unity will change the exact quantitative result. Conditions for pair production may also occur at similar laser intensities for a single laser beam incident on an overdense solid target. The incident and reflected laser beams form counterpropagating waves. Even if the laser beam is substantially absorbed rather than reflected, the electric field swells as the wave passes into the plasma and the phase velocity differs from the speed of light so that $\boldsymbol{E}$ and $\boldsymbol{\beta} \times \boldsymbol{B}$ are unlikely to cancel as in the unidirectional case. Furthermore, if the laser beam is in tight focus, as required for the highest intensities, it can be decomposed into obliquely propagating plane waves. Another factor favoring pair production is that the electrostatic field required for quasineutrality at a solid surface stops the electrons moving freely in the direction of laser propagation so that $\boldsymbol{E}$ and $\boldsymbol{\beta} \times \boldsymbol{B}$ once again cannot cancel, and the laser is able to play the role of particle accelerator and target simultaneously.

We predict that pair production should be a standard feature of laser-plasma interactions at intensities in the range 3×10^{23}–10^{24} W cm^{-2} at a laser wavelength of 1 μm. A significant number of pairs is produced at the lower end of this intensity range and the number increases dramatically when the intensity approaches 10^{24} W cm^{-2}. At intensities $\sim 10^{24}$ W cm^{-2} a cascade sets in, producing an avalanche which efficiently converts the laser energy into roughly equal numbers of pairs and γ rays. These predictions may be tested using high-power lasers in the next few years.

[1] J. Koga, T. Z. Esirkepov, and S. V. Bulanov, J. Plasma Phys. **72,** 1315 (2006).
[2] C. Müller, A. di Piazza, A. Shahbaz, T. J. Bürvenich, J. Evers, K. Z. Hatsagortsyan, and C. H. Keitel, Laser Phys. **18,** 175 (2008).
[3] J. Schwinger, Phys. Rev. **82,** 664 (1951).
[4] Y. I. Salamin, S. X. Hu, K. Z. Hatsagortsyan, and C. H. Keitel, Phys. Rep. **427,** 41 (2006).
[5] T. Erber, Rev. Mod. Phys. **38,** 626 (1966).
[6] A. K. Harding and D. Lai, Rep. Prog. Phys. **69,** 2631 (2006).
[7] J. K. Daugherty and I. Lerche, Phys. Rev. D **14,** 340 (1976).
[8] L. F. Urrutia, Phys. Rev. D **17,** 1977 (1978).
[9] E. P. Liang, S. C. Wilks, and M. Tabak, Phys. Rev. Lett. **81,** 4887 (1998).
[10] T. E. Cowan *et al.*, Laser Part. Beams **17,** 773 (1999).
[11] K. Nakashima, T. E. Cowan, and H. Takabe, in *Science of Superstrong Field Interactions*, edited by K. Nakajima and M. Deguchi, American Institute of Physics Conference Series (American Institute of Physics, Melville, NY, 2002), Vol. 634, pp. 323–328.
[12] D. L. Burke *et al.*, Phys. Rev. Lett. **79,** 1626 (1997).
[13] Y. Y. Lau, F. He, D. P. Umstadter, and R. Kowalczyk, Phys. Plasmas **10,** 2155 (2003).
[14] E. Brezin and C. Itzykson, Phys. Rev. D **2,** 1191 (1970).
[15] A. di Piazza, K. Z. Hatsagortsyan, and C. H. Keitel, Phys. Rev. Lett. **97,** 083603 (2006).
[16] L. D. Landau and E. M. Lifshitz, *The Classical Theory of Fields*, Course of Theoretical Physics-Pergamon International Library of Science, Technology, Engineering and Social Studies (Pergamon Press, Oxford, 1975), 4th revised English edition.
[17] A. di Piazza, Lett. Math. Phys. **83,** 305 (2008).
[18] Frequently also called *bremsstrahlung* [5], a term we reserve for radiation emitted in the electric field of a nucleus.
[19] F. A. Aharonian, *Very High Energy Cosmic Gamma Radiation: A Crucial Window on the Extreme Universe*, edited by F. A. Aharonian, Very High Energy Cosmic Gamma Radiation: A Crucial Window on the Extreme Universe (World Scientific Publishing, River Edge, NJ, 2004).